NASA Technical Paper 1475

Operating Condition and Geometry Effects on Low-Frequency Afterburner Combustion Instability in a Turbofan at Altitude

Richard R. Cullom and Roy L. Johnsen

JUNE 1979

NASA

NASA Technical Paper 1475

Operating Condition and Geometry Effects on Low-Frequency Afterburner Combustion Instability in a Turbofan at Altitude

Richard R. Cullom and Roy L. Johnsen
Lewis Research Center
Cleveland, Ohio

National Aeronautics
and Space Administration

**Scientific and Technical
Information Branch**

1979

SUMMARY

Altitude tests of three afterburner configurations were conducted with a low-bypass-ratio turbofan engine to determine the effect of fuel distribution, inlet conditions, flameholder and fuel injection system geometry on combustion instability. Flight conditions simulated for these tests were Mach 0.75 at altitudes from 11 580 to 12 800 meters (38 000 to 42 000 ft) and Mach 1.3 at altitudes from 12 190 to 14 020 meters (40 000 to 46 000 ft). The two experimental afterburner configurations which encountered combustion instability were partial forced mixers with V-gutter ring flameholders and multiple fuel spray bars. These two configurations differed in the axial location of the fuel bars. A number of different zone fuel distributions were tested to determine their effect on instability with these configurations. A production afterburner with a wider V-gutter ring flameholder was tested over the same range of conditions to determine its combustion characteristics.

In these tests afterburner combustion instability with frequency from 28 to 90 hertz and peak to peak pressure amplitudes up to 46.5 percent of the afterburner inlet total pressure level was encountered. For the afterburner configurations tested the instability amplitude generally increased as the fan stream fuel-air ratio increased and/or as the core stream fuel-air ratio decreased. The frequency of the instability increased as the afterburner inlet total pressure increased. At simulated flight conditions of Mach 1.28 and 12 170 meters (39 900 ft), the frequency of the instability decreased as the amplitude of the instability increased. At the conditions tested, the combustion instability could be suppressed by varying the afterburner fuel distribution. Values of combustion efficiency above 90 percent were recorded while operating with unstable afterburner combustion. Afterburner combustion efficiency generally decreased as the combustion instability amplitude increased.

INTRODUCTION

An investigation was conducted at the NASA Lewis Research Center with a full-scale turbofan engine to determine the effect of fuel distribution, inlet conditions and afterburner geometry on low frequency afterburner combustion instability. In the development of a turbofan or mixed-flow afterburner an operating problem which is usually encountered is a low frequency combustion instability. This instability is typically described as an axially traveling wave in the afterburner combustion section with a frequency from 30 to 300 hertz. This type of afterburner combustion instability is most

likely to occur in the subsonic, high-altitude portion of the aircraft flight envelope where the afterburner inlet pressure and fan stream temperatures are relatively low. A low amplitude instability can be tolerated as an irritant to the pilot of the aircraft but a higher amplitude instability can cause structural failure of the afterburner components. Low frequency afterburner combustion instability has been documented both in sea-level and flight tests (refs. 1 to 3). Although the instability has been documented, the cause of this type of instability is not well understood. The investigation reported herein presents instability data obtained over a range of controlled simulated flight conditions, zone fuel distributions, and for several afterburner configurations. By varying operational and geometric parameters and observing their effect on the combustion instability perhaps a better understanding of the instability phenomenon can be acquired. With improved understanding perhaps methods can be devised to suppress or eliminate the instability. The basic data can also be utilized in computer modeling of the combustion instability.

The afterburner-equipped engine was installed in an altitude test chamber and operated over a range of simulated flight conditions, nominal Mach numbers of 0.75 and 1.3 and altitudes from 11 580 to 14 020 meters (38 000 to 46 000 ft), to determine the effect of afterburner inlet conditions on combustion instability. Data were taken with a simulated higher turbine outlet temperature to investigate afterburner combustion instability characteristics in future higher turbine temperature turbofan engines. Three afterburner configurations were tested to evaluate the effect of flameholder geometry and fuel injection location on the instability characteristics. Also, differing zone fuel distributions were tested to assess their effect on the combustion instability.

APPARATUS

Engine

The engine type used for this investigation was a TF30-P-1 two-spool turbofan (fig. 1). The compressors, combustion section, and turbines were standard components. The three-stage axial-flow fan is mounted on the same shaft with a six-stage axial-flow low-pressure compressor. This assembly is driven by a three-stage low-pressure turbine. A seven-stage axial-flow high-pressure compressor is driven by a single-stage air-cooled high-pressure turbine. The compressor system overall pressure ratio is 17 to 1 and the fan pressure ratio of 2.1 to 1 with a fan bypass ratio of 1.0 at a sea-level static intermediate operating condition. A splitter ring divides the core and fan airflow at the exit of the third-stage rotor. The annular fan duct airflow combines with the turbine core flow in the afterburner diffuser. The combined flow discharges through a variable area exhaust nozzle.

Several modifications were made to these engines. At the turbine exit plane a multiple ring injector gaseous hydrogen burner was installed in an extended core duct section (fig. 1). This burner, shown in detail in figure 2, was used to reheat the turbine discharge flow and simulate operation of a higher turbine temperature turbofan engine. This hydrogen burner was supplied through three zone control valves which were manually regulated to obtain the desired temperature level and maintain a uniform radial profile. A screen of the correct porosity was installed in the fan duct to balance the pressure drop due to the hydrogen injectors in the core stream. The pressure drop balance between the core and fan streams maintained the heater-equipped engine on the standard engine operating line.

The standard integrated afterburner fuel flow-exhaust nozzle control was replaced with a simple exhaust nozzle area control. This control system varied the exhaust nozzle area to maintain the overall turbine pressure ratio. For these tests a manual fuel flow control system was provided for each afterburner zone.

Afterburner

The three afterburner configurations tested are described in the following sections.

P-3 afterburner. - The production TF30-P-3 afterburner consists of a diffuser section, combustion section, ring-type flameholders, and fuel spray rings (fig. 2). The flameholders and fuel spray rings are depicted in figure 3. The flameholder is a three-ring V-gutter type. Two of these rings, 3.6 centimeters (1.4 in.) in width, are mounted on the aft end of the diffuser cone with six radial gutters canted downstream. The third ring, 5.1 centimeters (2.0 in.) in width, was attached further upstream by a rod assembly to the diffuser cone. The flameholder array had a projected blockage of 38.3 percent of the net flow area inside the combustion section liner. As observed in figures 2 and 3, this blockage is not concentrated at a single axial location.

The seven fuel spray rings are arranged in five zones. Zone 1 consists of two spray rings designated zone 1 primary and zone 1 secondary. These two rings were fed through a fuel flow divider and individual manifolds. Zone 1 secondary is normally operated only at a main burner pressure greater than 124 newtons per square centimeter absolute (180 psia). Only the smaller diameter zone 1 primary spray ring was used for these tests. Zones 2, 3, and 4 are each single spray rings and inject fuel into the fan airflow. Zone 5 consists of two spray rings. Fuel from zones 1 and 5 is injected into the gas generator or core stream. The afterburner fuel is introduced progressively from zone 1 to 5 and the fuel flow was cumulative. For these tests the zone fuel flows were individually and manually controlled.

Mixer flameholder I. - An experimental configuration, a partial forced mixer with V-gutter ring flameholders and fuel spray bars is shown schematically in figure 4 and pictorially in figure 5. The mixer component consists of 20 fan-flow chutes (fig. 4(a)) and 20 core-flow chutes (fig. 4(b)). It was fabricated from nominally 0.122-centimeter- (0.048-in.-) thick Hastelloy X. The mixer is positioned such that the total fan airflow passes through the mixer fan chutes. The core chutes accommodate only a portion of the core flow. The ratio of the fan to core flow area at the exit plane of the mixer is 0.61. The flameholder consists of two ring V-gutters connected by 20 radial V-gutters (fig. 5). The radial V-gutters are positioned on the core chute centerlines at the exit of the mixer (fig. 4(b)). All flameholder V-gutter elements have an included angle of 45° and are 3.8 centimeters (1.5 in.) wide. The flameholder had a projected blockage of 38.8 percent.

Afterburner fuel is injected at two axial locations utilizing fuel spray bars arranged in five manually controlled zones. Fuel spray bars of Inconel 600 are 0.635 centimeter (0.25 in.) in diameter. The individual spray bars were assembled in groups of three bars. A complete description is given in table I. At the upstream locations 20 spray bar assemblies, each of two different injection hole patterns, were installed. The downstream location accommodated 20 spray bar assemblies. There is one spray bar assembly at the upstream location in the core chute (fig. 4(b)). There are two assemblies in each fan chute, one each at the upstream and downstream locations (fig. 4(a)). A total of 180 individual spray bars were installed. Fuel is injected perpendicular to the airflow. In figure 4, the cross-hatched sections of the spray bars indicate the length of the fuel injection regions.

Mixer flameholder II. - This experimental configuration differs from that of mixer flameholder I only in the axial location of the upstream fuel spray bar assemblies. For mixer flameholder II the 40 spray bar assemblies were moved downstream to the alternate location indicated in figure 4. The zone designations for the spray bar assemblies remained the same.

Installation

The installation of the engine in the altitude chamber, a conventional direct connect type, is shown in figure 6. Shown in the figure at the left is the forward bulkhead which separated the 5.5-meter- (18-ft-) diameter inlet plenum from the 7.3-meter- (24-ft-) diameter test chamber. Air of the required pressure and temperature flowed from the plenum at the left through the bellmouth into the engine inlet duct (fig. 1). A conical screen was attached to the bellmouth to prevent foreign object ingestion. A labyrinth seal, shown in figure 1, was used to isolate the inlet ducting from the bellmouth. A

seal, shown in figure 1, was used to isolate the inlet ducting from the bellmouth. A gimbal joint in the inlet ducting allowed free movement of the engine.

The engine was hung from an overhead mounting structure on the thrust bed (fig. 6). The thrust bed was suspended by four multiflexured vertical rods attached at their upper ends to the chamber. The bed alinement with the airflow direction was maintained by two multiflexured horizontal rods located fore and aft on the far side of the bed. The thrust bed was restrained from free movement by a dual load cell system that measured the thrust loads and allowed the bed to be preloaded.

Engine exhaust gases were captured by a moveable water-cooled collector extending from the rear bulkhead at the right. The collector minimized exhaust gas recirculation in the test chamber. A water-cooled periscope mounted in the exhaust duct was used to observe afterburner combustion.

Instrumentation

The instrumentation stations and probe locations corresponding to the installation in the engine and afterburner are shown in figures 1 and 2.

High-response pressure sensors and a strip chart recording system were used to measure the afterburner combustion instability amplitude and frequency. The location of these transient static pressure sensors is shown in figure 1. These sensors were flush mounted or close-coupled to wall static pressure taps. For the axial locations in the afterburner combustion section, these pressure taps were on the inside diameter of the cooling liner. This instrumentation system had a ±5 percent maximum amplitude error and was limited by the frequency response of the sensors to 300 hertz. Steady-state pressures were recorded by individual transducers and by 13 scanivalves (24 ports each) which were controlled by the facility computer. The differential-type scanivalve transducers were calibrated while in use and therefore had an estimated system accuracy of ±0.26 percent full scale. The individual differential-type transducer accuracy was ±0.60 full scale.

All thermocouples were a Chromel-Alumel type and were referenced to a 339 K (610° R) oven. Their estimated accuracy was ±1.1 K (2.0° R). Engine thrust and thrust bed preload forces were measured separately with 44 500-newton (10 000-lb) strain-gage-type load cells. The load cells were independently calibrated and mounted beneath the thrust bed. The basic thrust measuring system error was ±0.08 percent full scale.

The engine fuel flow was measured by two turbine-type flowmeters mounted in series. The engine fuel temperature was measured at the upstream flowmeter inlet. The afterburner total fuel flow was measured either with two low range turbine flow-

meters or two high range turbine flowmeters. The choice of measuring with the low or high flowmeter obviously depended on the fuel flow rate. This choice was controlled by a manually operated pneumatic selector valve. The afterburner zone fuel flows were individually measured with turbine flowmeters. The afterburner fuel temperature was measured at the inlet of the upstream flowmeter in the high flow run. The turbine flowmeters were individually calibrated and were accurate to ±0.56 percent full scale.

Procedure

Afterburner combustion instability tests were conducted at the following simulated flight conditions; nominal Mach numbers of 0.75 and 1.3 at altitudes from 11 580 to 14 020 meters (38 000 to 46 000 ft). At the selected Mach number and altitude the engine was accelerated to intermediate (highest nonafterburning) throttle position. For these tests the seventh- and twelfth-stage compressor bleeds were closed. The nonstandard exhaust nozzle area control was set to modulate the area to maintain the intermediate turbine pressure ratio as the afterburner zones were operated. Afterburner ignition was provided by the "hot streak" through the turbine technique. The afterburner fuel was introduced up to an overall fuel-air ratio of about 0.030. From this point the fuel flow was increased slowly as the afterburner was monitored for combustion instability. The signals from the high response pressure sensors mounted in the afterburner and fan duct were monitored on a visicorder for an increase in peak to peak amplitude above the usual combustion noise. Afterburner combustion characteristics were also observed through the exhaust nozzle opening by means of a television viewed periscope mounted downstream in the exhaust duct. High amplitude combustion instability was observed as a pulsation of the combustion plume. Also the thrust cell readings were unsteady during high amplitude instability. When a near uniform amplitude instability was observed, the afterburner fuel flow was held constant and data were recorded. Usually the time of operation in an unstable mode was limited to about 15 seconds to avoid fatigue damage to the flameholder and fuel manifolds. Return to stable combustion conditions was attained simply by decreasing the fuel flow. Fuel used in these tests was MIL-T-5624G grade JP-4.

Two TF30-P-1 engines were used in this test program. The first engine encountered a turbine section structural failure and was withdrawn from testing. This failure occurred while testing the mixing flameholder II configuration. The afterburner hardware and tailpipe were undamaged. This afterburner was mounted on a second engine and testing was continued. Comparison performance data of the mixer flameholder II obtained with the first and second engine were presented in reference 4 and show good agreement. Therefore it is felt that the results of the instability tests are not influ-

enced by this engine change. The first engine was used to test the production P-3 afterburner and mixer flameholders I and II. The second engine was used to complete testing of mixer flameholder II and for additional tests of mixer flameholder I.

DISCUSSION OF RESULTS

Combustion instability characteristics, frequency and pressure amplitude, will be presented for three afterburner configurations, the production P-3 and mixer flameholders I and II, at several simulated flight conditions. The two mixer flameholder configurations have different fuel injection locations so that the effect of fuel distribution and vaporization length on instability characteristics can be ascertained. Afterburner inlet pressure and temperature were varied to determine their effect on the instability characteristics. The effect of various afterburner zone fuel distributions on combustion instability will be discussed. Comparisons will be made between fuel distributions which results in combustion instabilities of varying amplitudes. Also presented are fuel distributions and a third afterburner configuration with a wider V-gutter flameholder, both of which produced stable combustion conditions. These comparisons of full-scale afterburner instability data should provide insight into the mechanisms which suppress or eliminate combustion instability. In the following discussion, low frequency afterburner combustion instability will be referred to as "rumble".

Fuel Distribution

The effect of zone fuel distribution on rumble will be discussed considering fan and core fuel-air ratios and the fuel vaporization rate within the fuel distribution. Proportioning of the total fuel flow through the afterburner zones appears to have some effect on the amplitude of the combustion instability. As the fuel flow to the fan stream was increased when the afterburner was operating near maximum thrust, references 1 and and 2 showed that the rumble amplitude increased. In the study reported herein, rumble characteristics, amplitude and frequency, will be recorded for various fan and core fuel-air ratios. The effect of different combinations of zone fuel flows on rumble intensity can then be determined for the particular afterburner configurations and conditions tested herein. An objective is to define fuel distributions which will suppress or eliminate the combustion instability.

An effect which may be inseparable from fuel distribution in a full-scale afterburner is the vaporization rate of the fuel. In a mixed-flow turbofan afterburner the bypassed fan airflow is at a relatively low temperature for engine operation at sub-

sonic Mach numbers and high altitudes. The low temperature of the fan airflow tends to limit the vaporization rate of the fuel injected into that stream. If fuel flows above this limiting rate are injected, liquid fuel droplets will be present in the airflow downstream of the flameholder. This, and sufficient available driving energy are conditions for rumble to occur as stated in reference 1. In this reference it was shown experimentally that slow, unsteady fuel vaporization rates contributed to unstable combustion in a mixed-flow afterburner.

In the study reported herein, changes in zone fuel distribution did affect the rumble intensity as indicated by the magnitude of the pressure instability amplitude. Whether the observed change in amplitude was due to a change in fuel vaporization rate because of the distribution change or whether it was simply due to the change in fuel distribution could not be determined.

Fuel distribution and rumble data were recorded at nominal simulated flight conditions of 1.29 Mach number at 12 160-meter (39 900-ft) altitude, conditions 1 to 6, table II and figure 7(a). Rumble with a 90-hertz frequency was encountered at condition 1 with mixer flameholder II. The pressure amplitude of the rumble was 9.4 percent, peak to peak, recorded at the flameholder location, station 8.08, figure 2. For condition 2, the fuel flow to the fan stream was increased. The rumble amplitude recorded at the flameholder increased to 14.2 percent peak to peak. The higher fuel flow to the fan stream probably provided more unvaporized fuel downstream of the flameholder and increased the rumble intensity. The decrease in core fuel-air ratio, decrease in zone 2 fuel flow, reduced the amount of fan stream heating and probably added to the rumble intensity. To isolate these two effects, in condition 3 the core fuel-air ratio was held constant and the fan fuel-air ratio was increased to 0.048. The rumble amplitude increased to 22.3 percent at the flameholder. Then for condition 4, the core fuel-air ratio was decreased to 0.020 while the fan fuel-air ratio was held nearly constant. The rumble amplitude increased to 35.4 percent, even though the overall fuel-air ratio decreased to 0.033. A large increase in the fan fuel flow (condition 5) produced severe rumble, 46.5 percent of the inlet pressure, at an overall fuel-air ratio of 0.037. At this condition the rumble frequency was 34 hertz. It is observed that the rumble amplitude increases if either the fan fuel-air ratio is increased or the core fuel-air ratio is decreased.

The variation of rumble amplitude with fan to core fuel distribution is illustrated in figure 8. The rumble amplitude is defined as the peak to peak variation in wall static pressure measured at the flameholder and expressed as a percent of the mixed total afterburner inlet pressure. The amplitude increases linearly over the range of fan to core fuel flow ratio investigated. It is observed that fuel distributions with increased fan fuel-air ratios increased the rumble intensity. Also distributions which

decrease the upstream core fuel flow also increased the rumble intensity for this mixer flameholder configuration.

If these observations of relating rumble intensity to the presence of unvaporized fuel downstream of the flameholder are correct, then it should be possible to suppress rumble by providing a pilot heat source to enlarge the recirculation zone at the flameholder and improve combustion conditions in the fan stream. Zone 3 is located in the fan stream immediately upstream of the flameholder. The zone 3 fuel flow was increased for condition 6 and provided rumble-free operation at a fuel-air ratio which resulted in severe rumble in condition 5. Comparison of conditions 5 and 6 in table II show the overall, core, and fan fuel-air ratios are the same. So the difference between severe rumble and stable combustion cannot be identified necessarily through overall fuel-air ratios, but detailed fuel distribution must be considered, especially where fuel is injected at different axial locations. In figure 7(a), it is seen that a redistribution of fan fuel flow from zone 4, condition 5, to zone 3 results in stable combustion for condition 6. This example shows how rumble can be suppressed through the use of zone 3 as a pilot zone to improve fan stream combustion conditions.

The observation that rumble can be suppressed under some conditions by proper fuel distribution is demonstrated at a higher altitude by comparing conditions 7 and 8. Rumble amplitude of 33.9 percent is recorded at the flameholder at an overall fuel-air ratio of 0.034 for condition 7. To suppress rumble, the fuel flows to zones 2 and 3 were increased for condition 8 (fig. 7(b)). The heat addition at the core upstream and fan downstream injection locations must assist in vaporizing the fuel, in addition to the piloting action of zone 3, because condition 8 was rumble-free at an overall fuel-air ratio of 0.043.

To further confirm the relation between piloting, low fuel vaporization rates, and the occurrence of rumble, stable combustion with mixer flameholder I was set (condition 9, table II and fig. 7(c)). Then the fuel flow to zone 3 was shutoff (condition 10). Even though the fan and overall fuel-air ratios decreased sharply, the afterburner rumbled. Zone 3 fuel flow was increased to 10 percent of the total afterburner fuel flow and additional fuel was injected into the fan stream at the upstream location (condition 11). The fan fuel-air ratio was 0.061 and no rumble was apparent. Thus it is observed that rumble can be suppressed if a fuel distribution which provides combustion piloting and an adequate fuel vaporization rate can be maintained.

Increased Turbine Outlet Temperature

If heat addition increases the fuel vaporization rates and suppresses rumble, perhaps future turbofans with higher turbine temperatures may not encounter as intense

rumble. An increased turbine outlet temperature will result in an increased core flow temperature and a higher afterburner mixed inlet temperature. Conditions 12 and 13 are presented to investigate the relation between inadequate fuel vaporization and rumble amplitude at higher afterburner inlet temperatures. Higher inlet temperature here is the result of simulating a higher turbine discharge temperature as provided by the hydrogen core gas heater (fig. 2). For these conditions the turbine discharge temperature has been raised by more than 170 K (300° F). Comparison can be made with similar fuel distributions at a lower inlet temperature to observe the effect of raising the turbine outlet temperature on rumble.

From the stable combustion of condition 12, rumble can be induced, as in condition 13, by decreasing the upstream core fuel flow and increasing the fan fuel flow. The overall fuel-air ratio was maintained constant. So the fuel distribution-afterburner rumble behavior described previously can also be encountered even at a higher turbine discharge temperature.

The question remains as to the effect of the higher turbine outlet temperature on the occurrence of rumble. This effect may be seen by comparing conditions 12 and 7. Percentage fuel distributions are the same for both conditions (fig. 7(b)). At the higher temperature, condition 12 is rumble-free at an overall fuel-air ratio of 0.038 and a fan fuel-air ratio of 0.048. Compared to condition 7 which is unstable at a fuel-air ratio of 0.034 and a lower fan fuel-air ratio. In this comparison the rumble-free operation of condition 12 may be attributed directly to the higher turbine outlet temperature.

The effect of the higher turbine temperature on rumble intensity can also be observed by comparing condition 13 with condition 14. Both conditions exhibit the same rumble amplitude. But with the higher inlet temperature (condition 13), this intensity rumble occurs at a higher overall fuel-air ratio, 0.037 compared to 0.033. These data also confirm the effectiveness of gas stream heating to aid fuel vaporization and reduce or eliminate rumble. From these comparisons, one concludes that, a mixer-type augmented turbofan engine with a higher turbine outlet temperature could extend the rumble-free operating regime of its afterburner.

While operating at condition 13, which produced rumble, the fuel flow to zone 5 was increased (condition 15). As the fan fuel-air ratio was increased the rumble of condition 13 diminished and the afterburner combustion became stable (condition 15). This is a reversal in parametric behavior from that shown in figure 8. The operating conditions and fuel distributions for these two conditions were compared in table II and figure 7(b). A possible explanation is that in condition 13 some of the fuel injected through zone 5 passes downstream of the flameholder unburned and provides energy to support rumble. As the zone 5 fuel flow was increased to condition 15, enough of the vaporized fuel forms a combustible mixture at the flameholder. This combustion probably acts similarly to the piloting action of zone 3 demonstrated in the section Fuel

Distribution. The pilot combustion in the fan stream tends to stabilize combustion by apparently enlarging the recirculation zone and providing heat to vaporize the fuel in the fan stream.

Vaporization Length

For the afterburner configuration operated at condition 5, the upstream spraybars were located 20.8 centimeters upstream of the flameholder face (fig. 4). This configuration and fuel distribution produced severe rumble. The same fuel distribution was operated in condition 11, but the fuel injection configuration was changed. The upstream spraybars, zones 2, 4, and 5, were now located further upstream, 30.5 centimeters from the flameholder face. Therefore the fuel vaporization length was increased from condition 5 to condition 11. No rumble was evident for condition 11, even though the overall fuel-air ratio was higher than for condition 5. Conditions 5 and 11 represent similar inlet conditions so the fuel vaporization rates should be similar from this standpoint. The 9.7 centimeter additional length between the fuel injection point and the flameholder location in condition 11 allows a greater percentage of the injected fuel to be vaporized. Apparently the improved fuel vaporization in condition 11 due to the increased vaporization length eliminates rumble for the same overall fuel-air ratio and inlet conditions.

Afterburner Inlet Conditions

The effect of varying the engine inlet and hence the afterburner inlet conditions on afterburner rumble frequency is considered in figure 9. Frequency data are presented over a range of inlet total pressures and temperatures corresponding to simulated flight Mach numbers 0.75 and 1.3, and altitudes from 11 580 to 14 020 meters (38 000 to 46 000 ft). The data were recorded with two configurations, mixer flameholders I and and II. Also, the hydrogen core heater was operated to raise the core stream temperature. The fuel distribution for all the data presented in figure 9 was approximately the same. The overall fuel-air ratio was approximately 0.035 and the core and fan ratios were 0.022 and 0.045, respectively.

All the data recorded with mixer flameholder II were obtained at a Mach number of 1.27 at altitudes of 12 190 and 14 020 meters (40 000 and 46 000 ft). So these data were obtained at the same inlet temperature. A trend of increasing rumble frequency with increased inlet pressure is indicated by the line drawn in figure 9.

The data obtained with mixer flameholder I were taken at Mach 0.75 at 11 580- and 12 190-meter (38 000- and 40 000-ft) altitude (conditions 16 to 21) and at Mach 1.32

at 12 440-meter (40 800-ft) altitude (condition 10). The inlet temperatures for the Mach 0.75 and 1.32 data were approximately 540 and 640 K (970° and 1160° R), respectively. Even though the inlet temperature varied, a trend of increased frequency with increased pressure is perceived. This trend is reasonable in light of the rumble frequency of 380 hertz at an inlet pressure of 2 atmospheres reported for a TF30 turbofan in reference 1.

The effect of afterburner inlet temperature on rumble frequency can be observed by comparing the data taken at an inlet pressure of approximately 7 newtons per square centimeter (10 psia). The data taken with mixer flameholder II at a mixed inlet temperature of 620 K (1120° R) exhibits a rumble frequency of 70 hertz. When the core hydrogen heater was in operation, the mixed inlet temperature was 700 K (1265° R) and the rumble frequency recorded was 89 hertz. From this limited data the rumble frequency may increase with increased inlet temperature.

Comparing the data recorded with the two afterburner configurations, mixer flameholder II exhibits a higher rumble frequency at a given inlet pressure. The only physical difference in these configurations is the distance from the upstream fuel injection station to the flameholder face, 30.5 to 20.8 centimeters. Therefore, the physical configuration of the afterburner, at least the fuel injection position, may affect the rumble frequency for a given inlet pressure. More data are needed to confirm this observation.

From figure 9 it is observed that the data corresponding to a given inlet condition, simulated flight Mach number and altitude, exhibit fairly constant values of instability frequency. This grouping of data can also be shown with a plot of rumble frequency against rumble amplitude (fig. 10). In this figure, mixer flameholder II at Mach 1.28 and 12 160 meters (39 900 ft) altitude displayed a rumble frequency of approximately 90 hertz at the lower values of rumble amplitude. For this afterburner configuration and operating condition the rumble frequency remained constant up to an amplitude of 25 percent. As the rumble intensity increases further, the frequency decreases sharply.

The data recorded at a Mach number of 0.75 display a rumble frequency of 28 hertz. The data for Mach 1.24 and 14 020-meter (46 000-ft) altitude show a rumble frequency of about 70 hertz. It appears that a unique value of rumble frequency is recorded at each simulated flight Mach number/altitude condition at the lower values of rumble amplitude. This unique value of rumble frequency could be referred to as the threshold rumble frequency corresponding to this particular Mach number/altitude condition. Because the threshold rumble frequency varies with Mach number/altitude, it must be a function of the afterburner inlet pressure and temperature. This can be verified by observing that the threshold frequency at Mach 1.24 and 14 020-meter (46 000-ft) altitude was increased from 70 to 90 hertz as the turbine outlet temperature is increased.

This situation was simulated by the operation of the core heater which raised the afterburner mixed inlet temperature and hence the threshold frequency.

Afterburner Combustion Efficiency

The variation of combustion efficiency, calculated from measured thrust, with fuel-air ratio is shown in figure 11. Data are presented for afterburner operation with stable combustion and in rumble to determine the effect of combustion instability on efficiency. The maximum value of efficiency was 93 percent recorded at a fuel-air ratio of 0.0345 with mixer flameholder II. A rumble amplitude of 14 percent of the afterburner inlet total pressure was recorded at this point. It is observed that operation in rumble at high values of efficiency is possible. From this operating point, the fuel flow to the fan stream was increased, raising the overall fuel-air ratio to 0.0355. Here the efficiency decreased to 91 percent as the rumble amplitude increased to 22 percent. The fan fuel flow was increased further to a fuel-air ratio of 0.0367. At this point, the efficiency decreased sharply to 70 percent. The afterburner was now operating in severe rumble with an amplitude of 47 percent of the inlet total pressure.

If the concept presented in reference 1 of slow, unsteady fuel vaporization rates contributing to rumble is considered, along with poor fuel distribution, the decrease in efficiency with increased rumble intensity can be explained. It is theorized that, as the fuel flow to the fan stream is increased, the injected fuel is not vaporized or is too lean to burn as it reaches the flameholder. This unvaporized fuel is not burned in the flameholder wake, thus decreasing efficiency, but passes downstream to be unsteadily burned, adding energy to the unstable combustion as evidenced by the increase in rumble amplitude. As the fan fuel flow was increased further, the fraction of unvaporized fuel increased, sharply decreasing the efficiency and increasing the rumble amplitude.

The concept of inadequate fuel vaporization/poor distribution can also be used to explain the rumble-free afterburner operation at higher fuel-air ratios. The severe rumble point at a fuel-air ratio of 0.0367 is condition 5. The rumble-free point at 0.0372 fuel-air ratio is condition 6. In table II the fuel-air ratios; overall, core, and fan, are the same for conditions 5 and 6. But the difference shown in figure 7(a) is an increased fuel flow to zone 3. Increased zone 3 fuel flow in condition 6 provided combustion piloting, raised the temperature of the fan stream and probably improved fuel vaporization thereby maintaining high combustion efficiency, 89 percent, and suppressing rumble.

The rumble-free point at a fuel-air ratio of 0.040 is condition 11 in table II and figure 7(c). The fuel distribution for condition 11 was similar to that of condition 5. But condition 11 was for mixer flameholder I and condition 5 was for mixer flame-

holder II. The difference between rumble-free and rumble operation can be explained on the basis of fuel vaporization. Mixer flameholder I had the upstream fan fuel injection station further upstream of the flameholder thereby increasing the fuel vaporization length. Here the increased length allowed improved fuel vaporization contributed to a high value of efficiency, 88 percent, and suppressed rumble.

Stable Combustion Configuration

In condition 22, the reference P-3 afterburner was operated at Mach 0.75 at 12 220-meter- (40 100-ft-) altitude at an overall fuel-air ratio similar to the ratios shown for the mixer flameholder I for conditions 19 to 21. The P-3 afterburner did not rumble at these conditions, whereas the mixer flameholder configuration did rumble at similar operating conditions (table II). The P-3 operated without rumble at condition 23, which was at a higher altitude and higher overall fuel-air ratio. Conditions 24 to 26 represent rumble-free operation from 12 to 13 600-meter- (40 to 45 000-ft-) altitude at overall fuel-air ratios up to 0.036. These stable combustion conditions were run so they compare to conditions 1 to 5, 10 and 7, recorded with mixer flameholders I and II which produced rumble at the same or lower overall fuel-air ratios.

Perhaps the stable combustion of the P-3 afterburner can be partially attributed to the fuel distribution. For conditions 22 to 26 the fan fuel-air ratio was always lower than the core fuel-air ratio. It was shown in condition 4 that a decrease in core fuel-air ratio increased the rumble amplitude. Conversely, if the core fuel flow was increased, the rumble intensity should diminish. Also, it was shown, in most cases, that high fan fuel-air ratios intensified the rumble (fig. 8). Thus, from the observations here, to suppress rumble, a fuel distribution with a fan to core fuel ratio near unity should be considered for turbofan engines in this bypass ratio range. So the standard P-3 fuel distribution probably contributes to its rumble-free operation.

Another significant difference between the P-3 and the mixer flameholder configuration is the blockage characteristics of the flameholder. The total blockage of the two flameholder configurations was similar, the P-3 equaled 38.3 percent and the mixer flameholder was 38.8 percent. But the main flameholder ring in the P-3 configuration is 5.1 centimeters (2.0 in.) wide, whereas the width of the flameholder rings used with the mixer are 3.8 centimeters (1.5 in.). Perhaps the wider V-gutter provides a more stable recirculation zone which penetrates further downstream. The greater axial length recirculation zone may enhance the possibility of entraining and burning unvaporized fuel if it is present downstream of the flameholder. So if rumble is intensified by unvaporized fuel downstream of the flameholder, the wider V-gutter/ longer recirculation zone may reduce the amount of unvaporized fuel and thereby sup-

press rumble. Therefore, the pertinent consideration with regard to rumble may not be total blockage per se, but how that blockage is distributed in the flameholder design.

SUMMARY OF RESULTS

Altitude tests of a low-bypass-ratio augmented turbofan engine were conducted to investigate low-frequency afterburner combustion instability. The following results were obtained for the configurations tested:

1. Afterburner combustion instability with frequency from 28 to 90 hertz and peak to peak pressure amplitudes up to 46.5 percent of the afterburner inlet total pressure was encountered.

2. For the afterburner configurations tested, the amplitude of the instability generally increased as the fan fuel-air ratio increased and/or as the core fuel-air ratio decreased.

3. Combustion instability frequency increased as the afterburner inlet total pressure increased.

4. At simulated flight conditions of Mach number 1.28 and 12 170 meter (39 900-ft) altitude, the combustion instability frequency decreased as the amplitude of the instability increased.

5. Increasing the fuel vaporization length eliminated combustion instability at comparable fuel-air ratios and inlet conditions tested herein.

6. For the conditions tested, combustion instability was suppressed by providing combustion piloting and heating the fan fuel-air flow to improve fuel vaporization.

7. Other things being equal, a mixer-type augmented turbofan engine with a higher turbine outlet temperature could extend the stable combustion operating regime of its afterburner.

8. Afterburner combustion efficiency generally decreased as the combustion instability amplitude increased.

9. Values of combustion efficiency above 90 percent were recorded while operating with unstable combustion.

10. A triple ring-type afterburner configuration with equal total blockage and a 5.1-centimeter- (2.0-in.-) wide ring V-gutter was stable at all operating conditions investigated which produced combustion instability with a mixer-type afterburner with 3.8-centimeter (1.5-in.) V-gutters.

Lewis Research Center,
National Aeronautics and Space Administration,
Cleveland, Ohio, February 23, 1979,
505-04.

REFERENCES

1. Smith, George E.; and Henderson, Robert E.: Combustion Instability in a Turbofan Mixed-Flow Augmentor. Presented at the Low Frequency Combustion Instability Seminar, Air Force Aero Propulsion Lab., (Wright-Patterson AFB, Ohio), May 21, 1975. (Also AIAA Paper 72-1206, Nov. 1972.)

2. Rusnak, J.: Low Frequency Combustion Instability Experience at Pratt & Whitney Aircraft. Presented at the Low Frequency Combustion Instability Seminar, Air Force Propulsion Lab., (Wright-Patterson AFB, Ohio), May 21, 1975.

3. Johnson, Thomas: A 50 hz Combustion Instability in the RM8A Turbofan Augmentor. Presented at the Low Frequency Combustion Instability Seminar, Air Force Aero Propulsion Lab., (Wright-Patterson AFB, Ohio), May 21, 1975.

4. Johnsen, Roy L.; and Cullom, Richard R.: Altitude Test of Several Afterburner Configurations on a Turbofan Engine With a Hydrogen Heater to Simulate an Elevated Turbine Discharge Temperature. NASA TP-1068, 1977.

TABLE I. - SPECIFICATIONS FOR TWO AFTERBURNER CONFIGURATIONS, MIXER FLAMEHOLDERS I AND II

Fuel zone	Manifold type	Number of holes per bar	Hole diameter, cm	Injection location	Reference figure
1	20 Radial bars	3	0.0635	Core, downstream	4(a)
2	20 Radial bars	3	.0572	Core, upstream	4(a)
	20 Radial bars	5	.0572	Core, upstream	4(b)
3	20 Radial bars	6	.0572	Fan, downstream	4(a)
4	20 Radial bars	4	.0572	Fan, upstream	4(a)
	20 Radial bars	2	.0572	Fan, upstream	4(b)
5	20 Radial bars	6	.0635	Fan, upstream	4(a)
	20 Radial bars	2	.0635	Fan, upstream	4(b)

TABLE II. - TEST CONDITIONS AND AFTERBURNER COMBUSTION INSTABILITY DATA

Condition number	Afterburner configuration	Flight Mach number	Altitude		Afterburner inlet conditions (Station 7.5)								Afterburner fuel-air ratios			Combustion instability data			
			m	ft	Mixed total pressure		Mixed total temperature		Core flow temperature		Fan flow temperature		Overall	Core	Fan	Frequency, Hz	Peak-to-peak amplitude in percent of inlet total pressure at -		
					N/cm abs	psia											Fan duct	Station 8.06	Station 8.64
1	Mixer flame-holder II	1.29	11 980	39 300	11.05	16.02	631	1136	904	1628	400	720	0.034	0.028	0.041	90	10.0	9.4	9.4
2		1.27	12 160	39 900	10.69	15.50	640	1152	898	1618	400	720	.035	.024	.046	83	13.5	14.2	----
3		1.29	12 190	40 000	10.83	15.70	641	1154	909	1636	400	721	.036	.024	.048	90	19.1	22.3	22.3
4		1.31	12 320	40 400	10.71	15.52	643	1157	904	1628	400	720	.033	.020	.047	80	30.3	35.4	32.2
5		1.30	12 250	40 200	10.37	15.03	634	1142	882	1589	398	717	.037	.019	.056	34	38.6	46.5	36.6
6		1.28	12 040	39 500	10.74	15.57	637	1147	890	1603	397	714	.037	.019	.056	0	0	0	0
7		1.23	14 020	46 000	7.12	10.32	624	1123	890	1603	393	707	.034	.025	.044	72	29.1	33.9	11.6
8		1.22	13 870	45 500	7.15	10.37	649	1168	904	1628	391	704	.043	.039	.046	0	0	0	0
9	Mixer flame-holder I	1.21	12 100	39 700	10.93	15.85	645	1161	902	1623	396	712	.036	.019	.053	0	0	0	0
10		1.32	12 440	40 800	10.77	15.62	645	1161	898	1618	397	715	.032	.019	.046	75	16.0	32.0	16.0
11		1.22	12 040	39 500	11.00	15.94	644	1159	906	1630	395	711	.040	.020	.061	0	0	0	0
12	Mixer flame-holder II	1.22	13 900	45 600	7.04	10.20	704	1267	1096	1973	393	708	.038	.026	.048	0	0	0	0
13		1.23	13 930	45 700	7.06	10.23	702	1265	1094	1970	393	707	.037	.022	.051	89	19.5	22.5	----
14		1.24	14 020	46 000	7.23	10.48	622	1120	889	1600	393	707	.033	.021	.046	70	19.1	21.9	----
15		1.22	13 870	45 500	7.02	10.17	708	1274	1106	1990	393	707	.043	.023	.060	0	0	0	0
16	Mixer flame-holder I	.75	11 620	38 100	6.10	8.84	534	962	747	1345	333	600	.032	.024	.042	28	22.6	22.6	17.0
17		.75	11 680	38 300	6.03	8.74	534	961	748	1347	334	601	.033	.025	.043	28	22.9	28.6	22.9
18		.75	11 550	37 900	5.90	8.55	544	979	755	1359	332	597	.038	.024	.052	25	17.5	23.4	17.5
19		.75	12 220	40 100	5.59	8.11	539	970	753	1356	333	600	.033	.025	.043	28	24.7	28.4	24.7
20		.76	12 260	40 200	5.55	8.05	539	970	754	1358	333	600	.033	.024	.043	28	18.6	24.9	18.6
21		.77	12 190	40 000	5.57	8.08	---	----	----	----	---	---	.035	.025	.045	28	24.8	31.0	24.8
22	TF30-P-3	.75	12 220	40 100	5.77	8.37	548	987	766	1378	332	598	.034	.036	.033	0	0	0	0
23		.75	12 830	42 100	4.99	7.24	542	975	758	1364	331	595	.041	.043	.040				
24		1.28	12 070	39 600	10.62	15.40	642	1156	890	1603	394	710	.036	.038	.036				
25		1.23	13 170	43 200	8.24	11.94	640	1152	890	1603	393	707	.036	.039	.035				
26		1.21	13 600	44 600	7.14	10.36	634	1141	880	1584	389	701	.035	.037	.034				

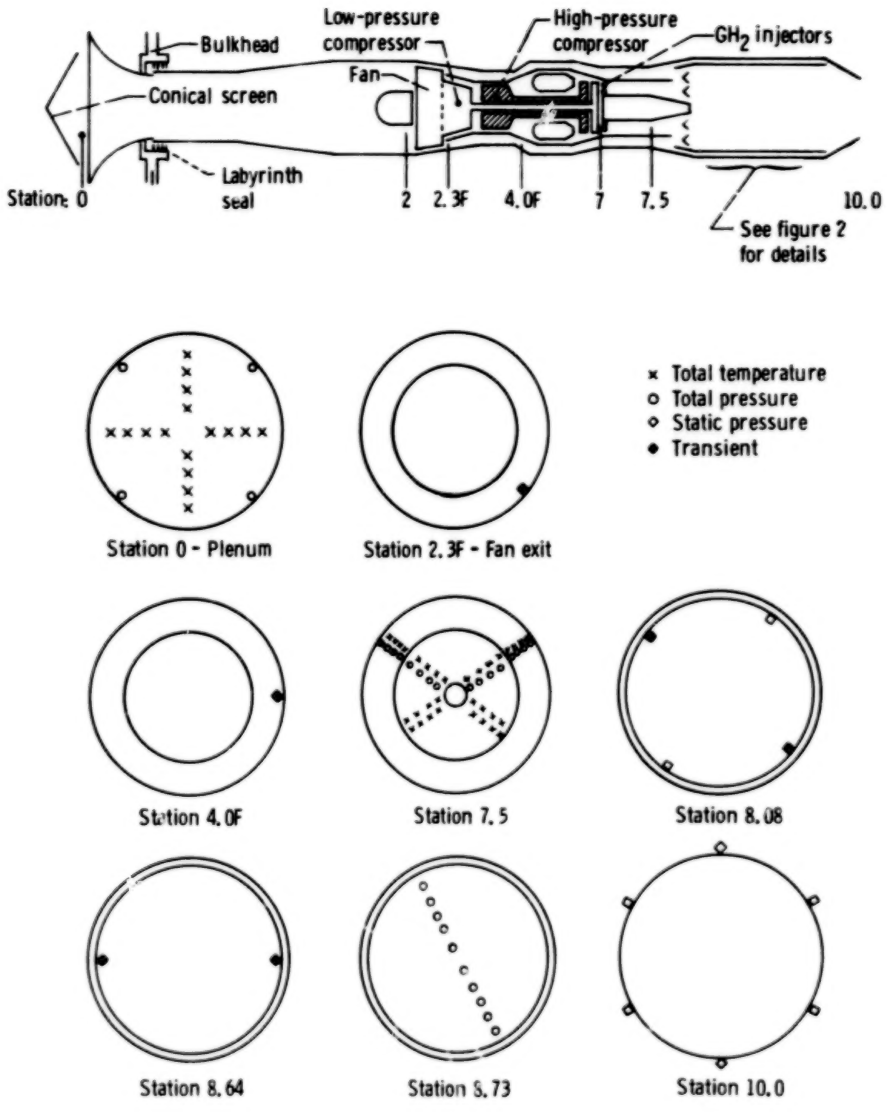

Figure 1. - Instrumentation layout (stations viewed looking upstream).

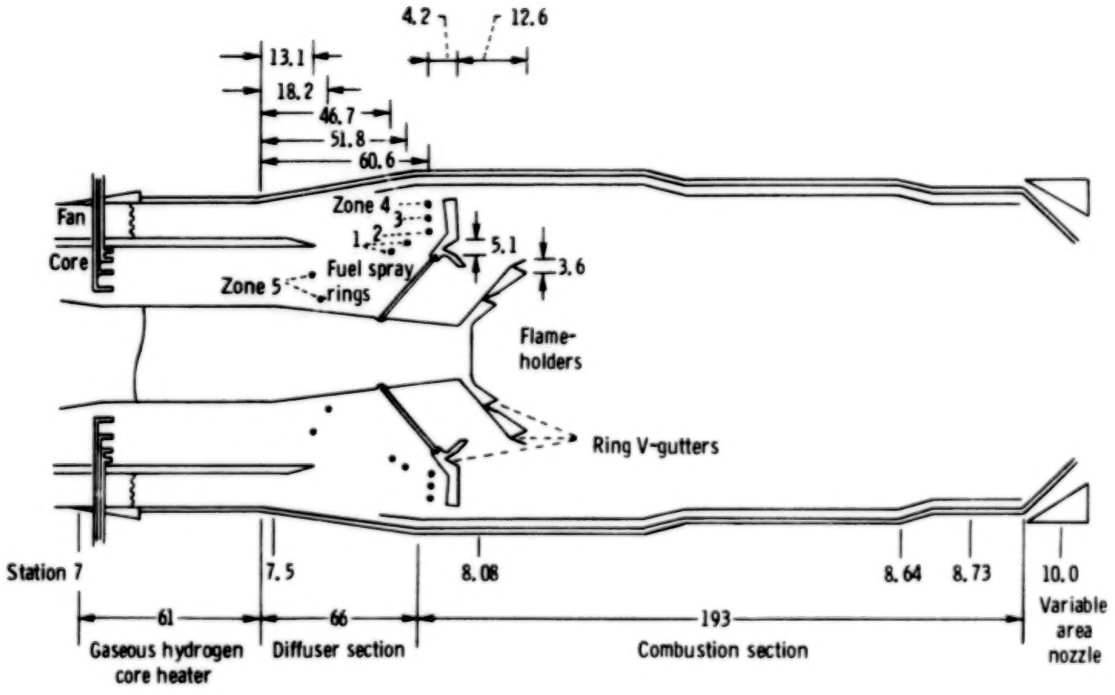

Figure 2. - Cross-sectional schematic of P-3 afterburner with instrumentation stations. (All dimensions in cm.)

Figure 3. - Flameholder and fuel manifold for TF30-P-3 afterburner.

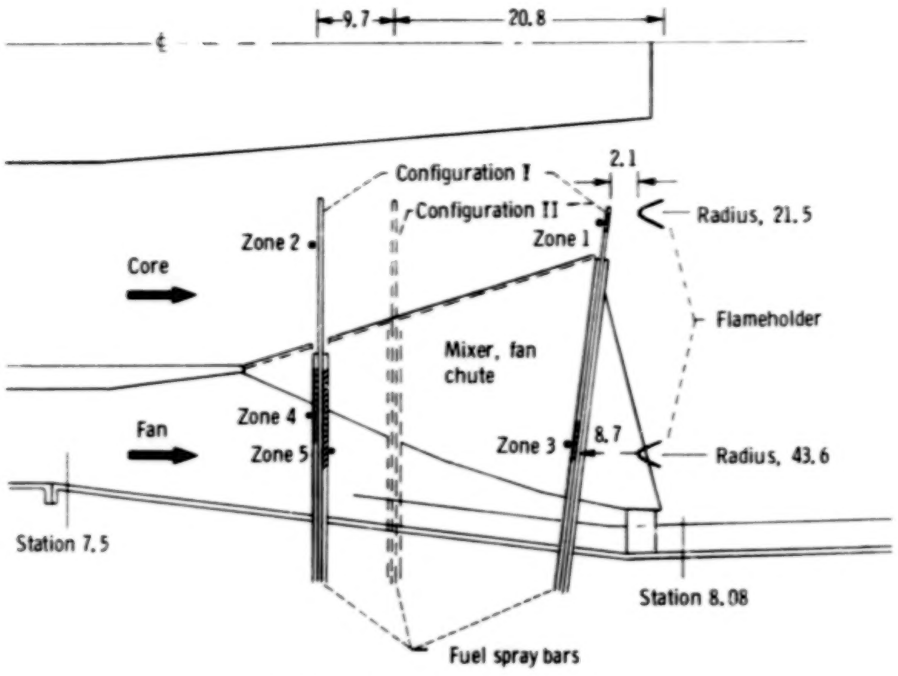

(a) Section on mixer fan chute centerline.

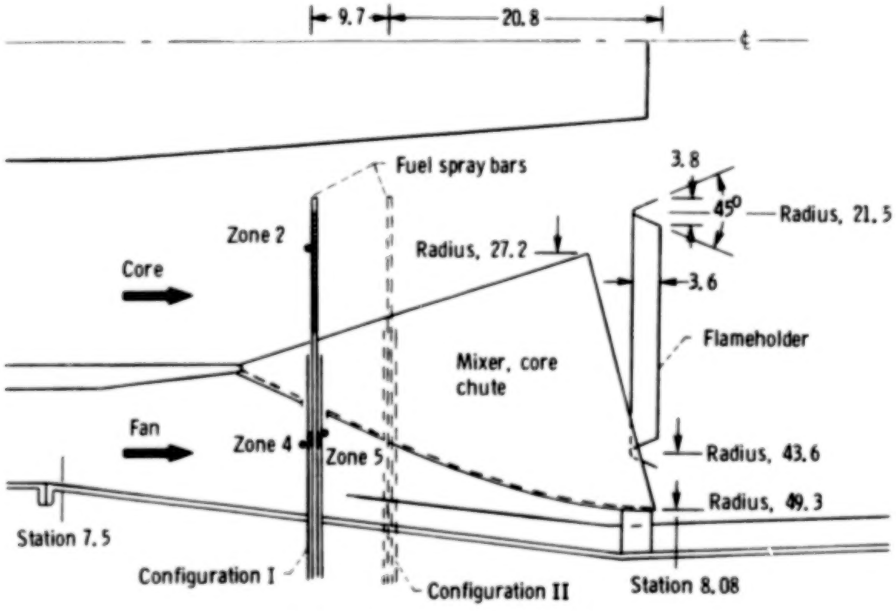

(b) Section on mixer core chute centerline.

Figure 4. - Cross-sectional schematic of mixer flameholder afterburner; configurations I and II. (Dimensions in cm unless indicated otherwise.)

Figure 5. - Mixer flameholder viewed from aft. Core and fan chutes and the radial fuel bars are shown.

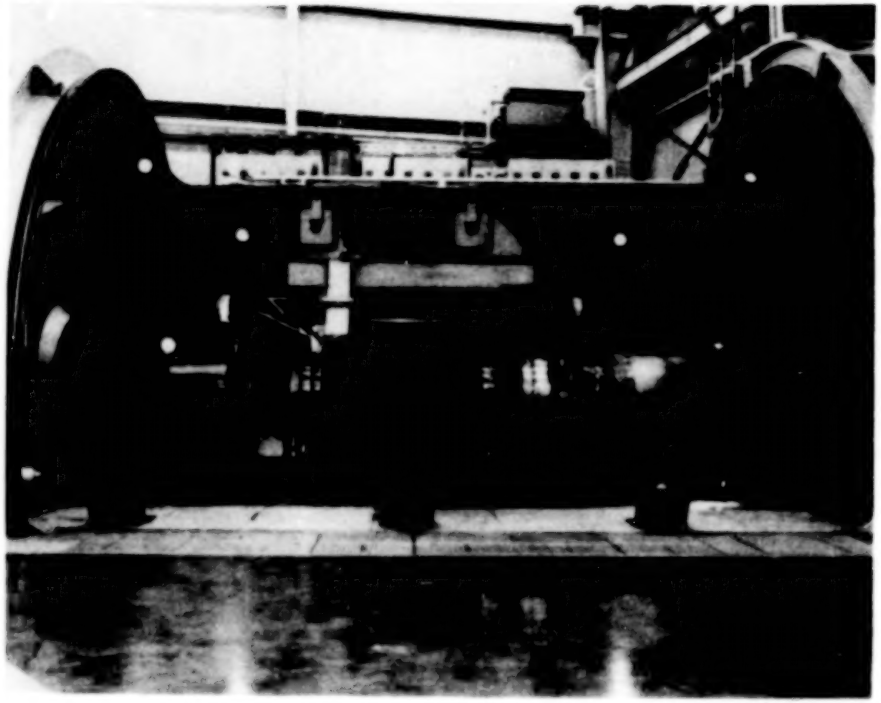

Figure 6. - Turbofan engine installed in altitude test chamber.

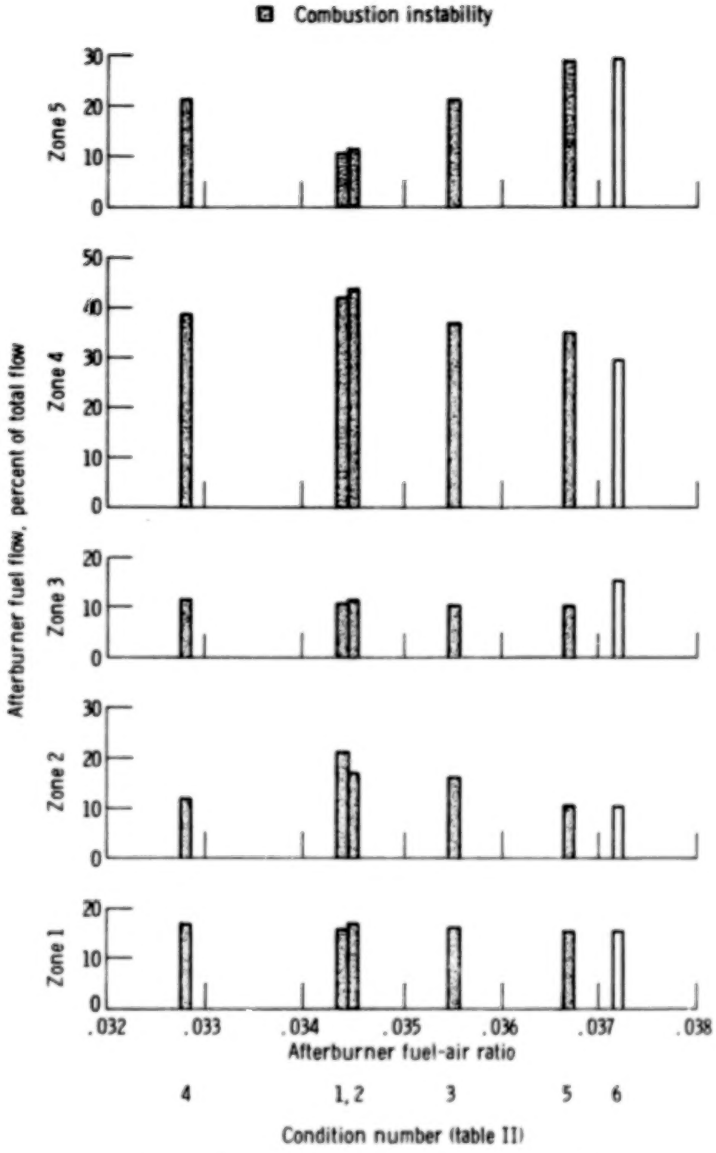

(a) Mixer flameholder II; average simulated flight conditions; Mach number, 1.29; altitude, 12 160 m (39 900 ft).

Figure 7. - Afterburner fuel distribution.

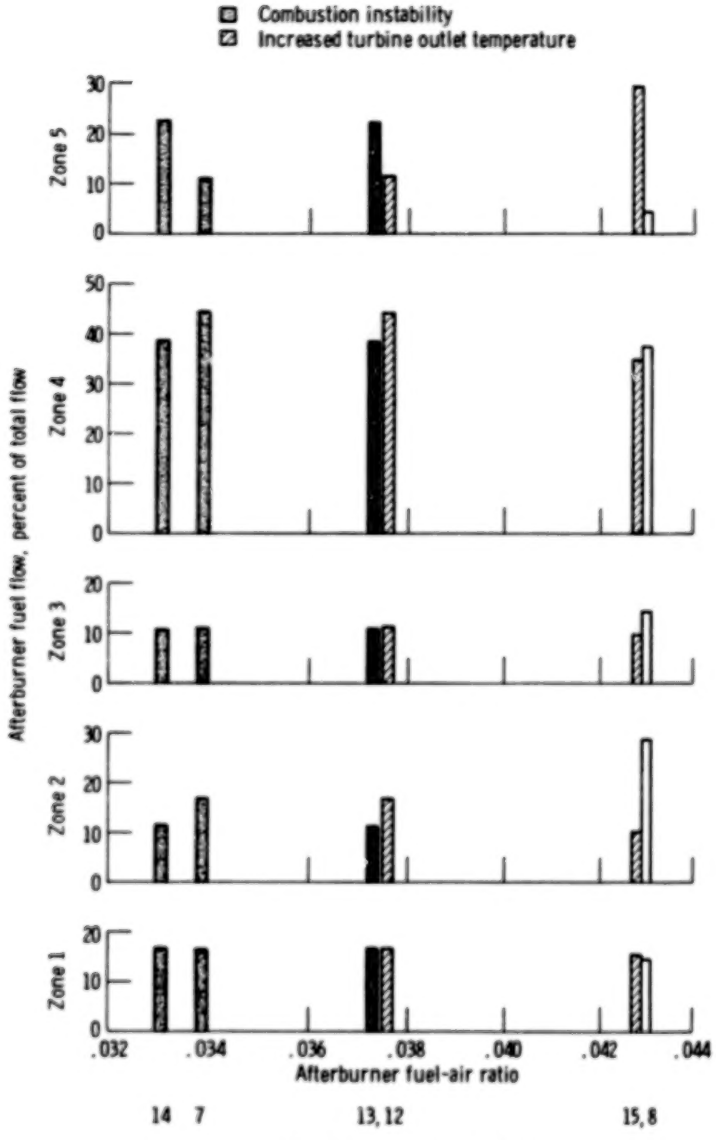

(b) Mixer flameholder II; average simulated flight conditions; Mach number, 1.23; altitude, 13 930 m (45 700 ft).

Figure 7. - Continued.

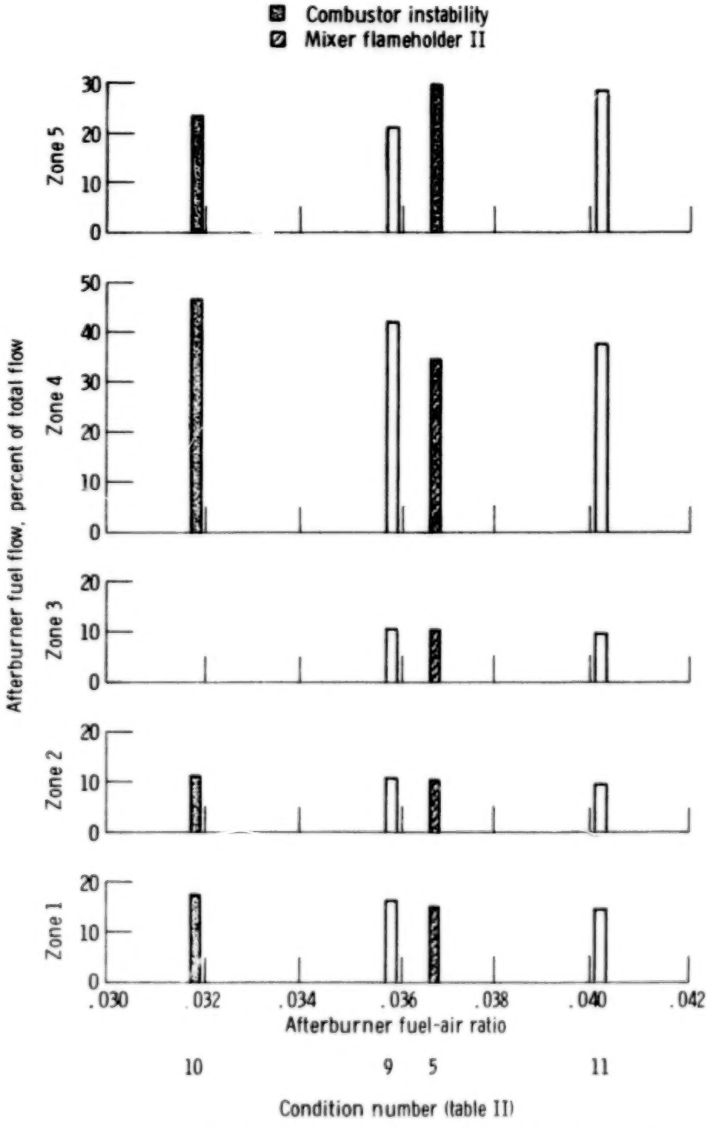

(c) Mixer flameholder I and II; average simulated flight conditions; Mach number, 1.26; altitude, 12 230 m (40 100 ft).

Figure 7. - Continued.

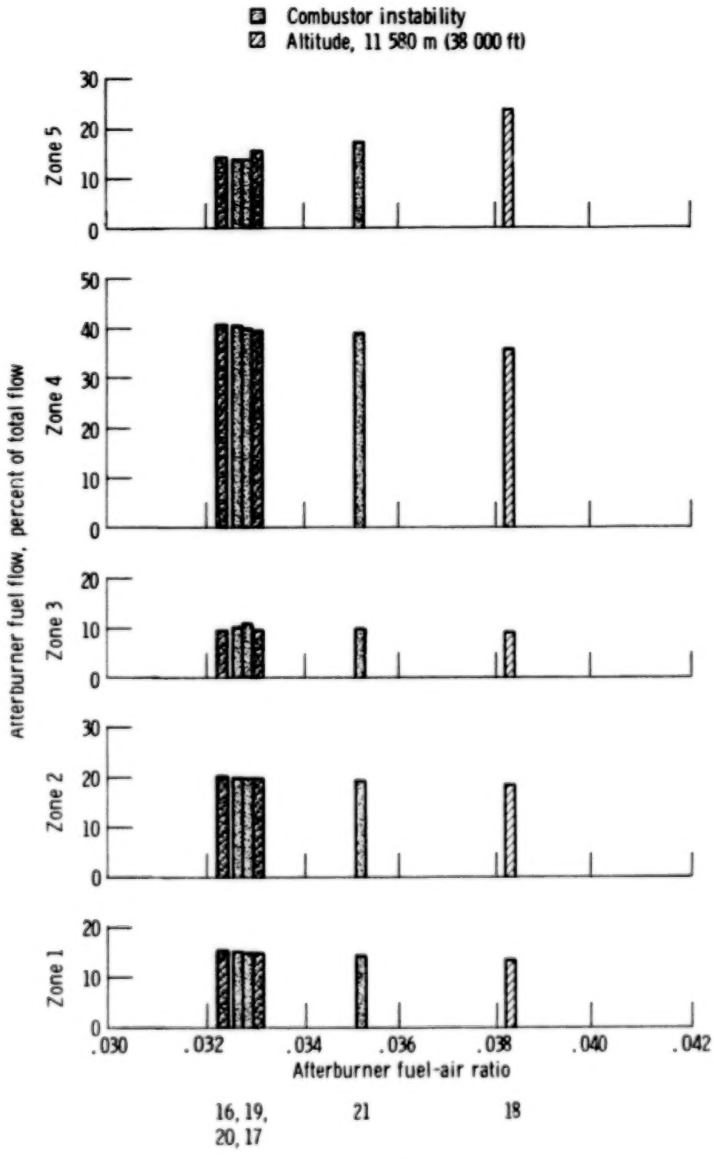

(d) Mixer flameholder I; average simulated flight conditions; Mach number, 0.76; altitude, 11 580 and 12 190 m (38 000 and 40 000 ft).

Figure 7. - Concluded.

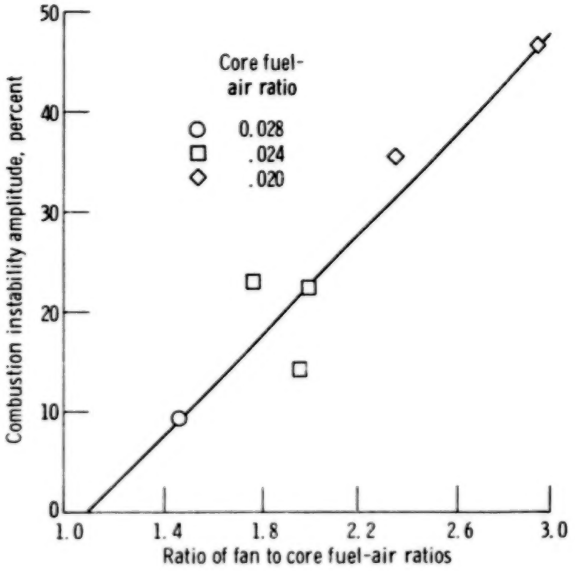

Figure 8. - Combustion instability amplitude as a function of fuel distribution. Mixer flameholder II; Mach number, 1.29; Altitude, 12 160 m (39 900 ft).

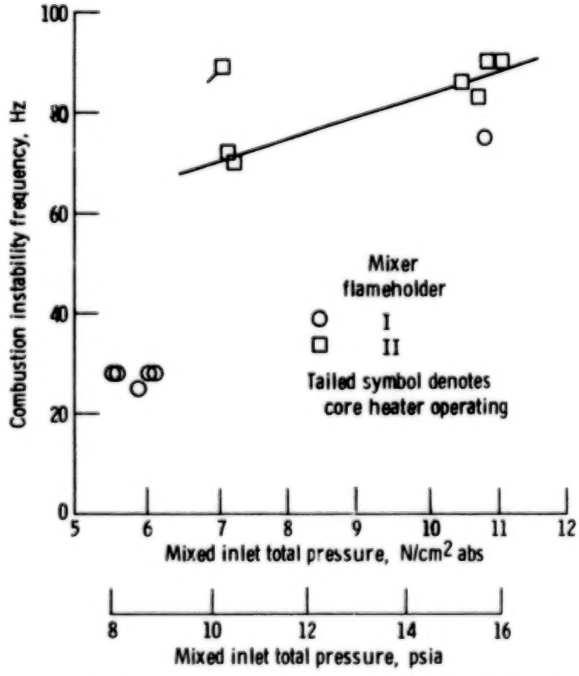

Figure 9. - Combustion instability frequency against inlet total pressure.

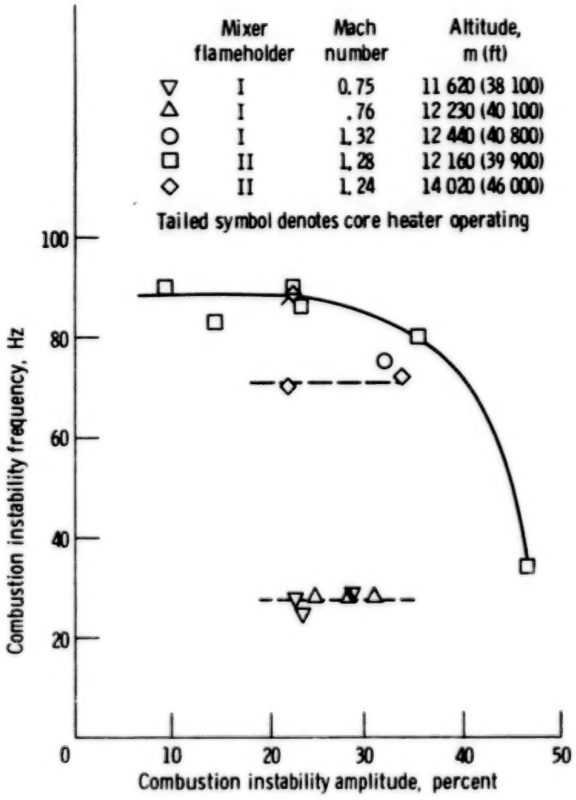

Figure 10. - Combustion instability frequency plotted against amplitude.

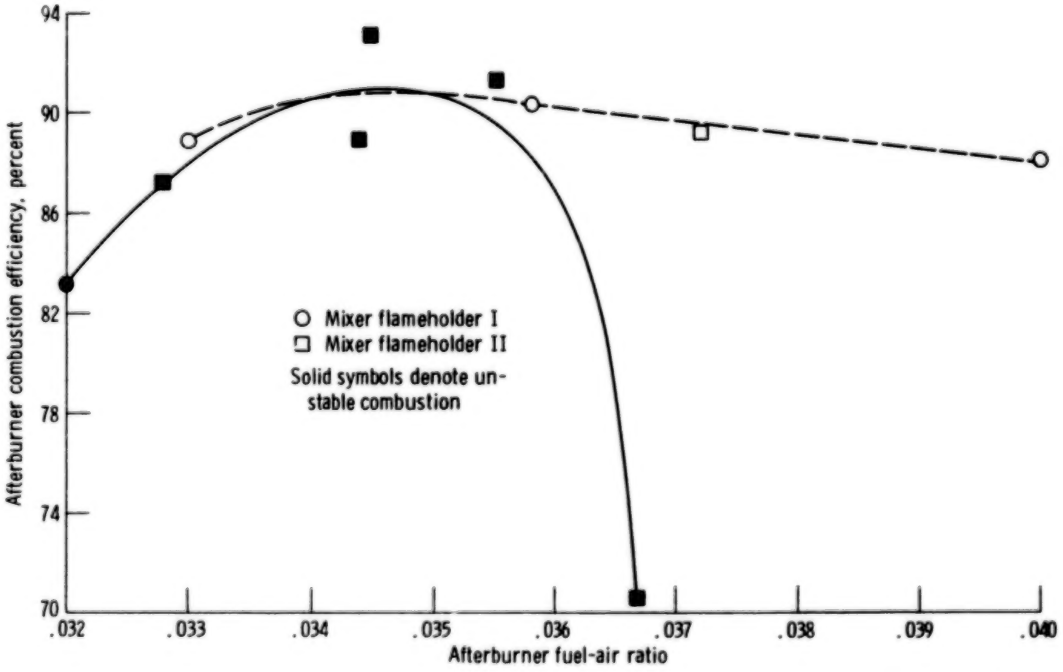

Figure 11. - Effect of combustion instability on combustion efficiency. Mach number, 1.28; altitude, 12 160 m (39 900 ft).

1. Report No.	2. Government Accession No.	3. Recipient's Catalog No.
NASA TP-1475		

4. Title and Subtitle	5. Report Date
OPERATING CONDITION AND GEOMETRY EFFECTS ON LOW-FREQUENCY AFTERBURNER COMBUSTION INSTABILITY IN A TURBOFAN AT ALTITUDE	June 1979
	6. Performing Organization Code
7. Author(s) Richard R. Cullom and Roy L. Johnsen	8. Performing Organization Report No. E-9886
	10. Work Unit No. 505-04
9. Performing Organization Name and Address National Aeronautics and Space Administration Lewis Research Center Cleveland, Ohio 44135	11. Contract or Grant No.
	13. Type of Report and Period Covered Technical Paper
12. Sponsoring Agency Name and Address National Aeronautics and Space Administration Washington, D.C. 20546	14. Sponsoring Agency Code

15. Supplementary Notes

16. Abstract

Three afterburner configurations were tested in a low-bypass-ratio turbofan engine to determine the effect of various fuel distributions, inlet conditions, flameholder geometry, and fuel injection location on combustion instability. Tests were conducted at simulated flight conditions of Mach 0.75 and 1.3 at altitudes from 11 580 to 14 020 m (38 000 to 46 000 ft). In these tests combustion instability with frequency from 28 to 90 Hz and peak-to-peak pressure amplitude up to 46.5 percent of the afterburner inlet total pressure level was encountered. Combustion instability was suppressed in these tests by varying the fuel distribution in the afterburner.

17. Key Words (Suggested by Author(s))	18. Distribution Statement
Afterburner; Augmentor; Mixed-flow afterburner; Mixer flameholder; Ring flameholder; Rumble; Afterburner combustion instability; Low-frequency combustion instability	Unclassified - unlimited STAR Category 07

19. Security Classif. (of this report)	20. Security Classif. (of this page)	21. No. of Pages	22. Price*
Unclassified	Unclassified	30	A03

* For sale by the National Technical Information Service, Springfield, Virginia 22161

NASA-Langley, 1979

29

90 %